Anal. Chem. **2009,** *81,* 8365–8372

Dependence of Antimicrobial Selectivity and Potency on Oligomer Structure Investigated Using Substrate Supported Lipid Bilayers and Sum Frequency Generation Vibrational Spectroscopy

Christopher W. Avery,[†] Abhigyan Som,[‡] Yongjiang Xu,[§] Gregory N. Tew,[‡] and Zhan Chen*[,†]

Department of Chemistry, University of Michigan, Ann Arbor, Michigan 48109, Department of Polymer Science and Engineering, University of Massachusetts, Amherst, Massachusetts 01002, and PolyMedix, Inc., Radnor, Pennsylvania 19087

Sum frequency generation (SFG) vibrational spectroscopy was used to study interactions between solid-supported lipid bilayers mimicking microbial and erythrocyte cellular membranes and synthetic antimicrobial arylamide oligomers named 2, 3, and 4, designed with the facial amphiphilicity common to naturally occurring antimicrobial peptides. The three compounds have the same backbone structure but varied side chains. The inherent interfacial sensitivity of SFG allowed for simultaneous monitoring of lipid ordering in the individual bilayer leaflets and orientation of 2, 3, and 4 upon interaction with the bilayer. Critical concentrations at which the inner leaflet is disrupted were determined for each oligomer. Spectral evidence of the oligomers' interaction with the bilayer below the critical concentrations was also found. Oligomers 2 and 3 tilted toward the bilayer surface normal, in agreement with previous experimental and simulation results. These oligomers selectively interact with microbial membrane models over erythrocyte membrane models, correlating well to previously published SFG studies on antimicrobial oligomer 1. It was shown that the oligomers interact with the lipid bilayers differently, indicating their different activity and selectivity. This research further shows that SFG is a particularly useful technique for the investigation of interaction mechanisms between cell membranes and membrane-active molecules. Additionally, SFG provides details of the specific interactions between these novel antimicrobials and lipid bilayers.

Since the 1930s, with the introduction of sulfonamide drugs for therapeutic applications, antibiotics have become widely used as highly effective tools to combat infectious diseases. However, since their introduction into the standard medical arsenal, bacteria have been developing resistance to many antibiotics. Resistant strains are now commonly seen in hospitals, and very few solutions for solving this problem have yielded significant results. As a result, antibiotic resistance is becoming regarded as a massive threat to global public health, and investigation into new antibiotics is drawing new levels of interest.[1]

Antimicrobial peptides (AMPs) represent a particularly interesting new perspective in the development of new drugs.[1−6] AMPs have large structural diversity and broad-spectrum applicability, but what makes them most interesting is that they have a unique mode of action: they target the lipid membrane itself, rather than proteins or specific receptors contained within the membrane or inside the cell.[1−6] This effectively minimizes any drug resistance ability of the microbe against AMPs. However, AMPs are inherently complex, and before they could be used in any effective manner, the mechanisms by which they work should be better understood. Extensive research has been performed to understand such mechanisms.[1−6]

It was demonstrated in previous work that simple structures can be made as effective mimics for AMPs, intentionally designing them to have the same potent broad-spectrum activity as their natural counterparts.[7−9] Additionally, it was shown that these molecules can differentiate between microbial and erythrocyte cellular membrane models. Molecular dynamics simulations showed that molecules with a facially amphiphilic structure similar to those shown in Figure 1 would have a molecular plane perpendicular to the bilayer plane, thus inserting into the bilayer similar to a knife cutting into cheese.[10] These simulations were confirmed by direct experimental evidence using SFG vibrational spectroscopy.[11]

* To whom all correspondence should be addressed. E-mail: zhanc@umich.edu. Fax: 734-647-4685.
† University of Michigan.
‡ University of Massachusetts.
§ PolyMedix, Inc.

(1) Zasloff, M. *Nature* **2002**, *415*, 389–395.
(2) Matsuzaki, K. *Biochim. Biophys. Acta* **1999**, *1462*, 1–10.
(3) Hancock, R. E. W.; Diamond, G. *Trends Microbiol.* **2000**, *8*, 402–411.
(4) Epand, R. M.; Vogel, H. J. *Biochim. Biophys. Acta* **1999**, *1462*, 11–28.
(5) Sitaram, N.; Nagaraj, R. *Biochim. Biophys. Acta* **1999**, *1462*, 29–54.
(6) Brogden, K. A. *Nat. Rev. Microbiol.* **2005**, *3*, 238–250.
(7) Tew, G. N.; Liu, D.; Chen, B.; Doerksen, R. J.; Kaplan, J.; Carroll, P.; Klein, M. L.; DeGrado, W. F. *Proc. Natl. Acad. Sci. U.S.A.* **2002**, *99*, 5110–5114.
(8) Yang, L.; Gordon, V. D.; Mishra, A.; Som, A.; Purdy, K. R.; Davis, M. A.; Tew, G. N.; Wong, G. C. L. *J. Am. Chem. Soc.* **2007**, *129*, 12141–12147.
(9) Yang, L.; Gordon, V. D.; Trinkle, D. R.; Schmidt, N. W.; Davis, M. A.; DeVries, C.; Som, A.; Cronan, J. E., Jr.; Tew, G. N.; Wong, G. C. L. *Proc. Natl. Acad. Sci. U.S.A.* **2008**, *105*, 20595–20600.
(10) Lopez, C. F.; Nielson, S. O.; Moore, P. B.; Klein, M. L. *Proc. Natl. Acad. Sci. U.S.A.* **2004**, *101*, 4431–4434.
(11) Chen, X.; Tang, H.; Even, M. A.; Wang, J.; Tew, G. N.; Chen, Z. *J. Am. Chem. Soc.* **2006**, *128*, 2711–2714.

10.1021/ac901271f CCC: $40.75
Published on Web 09/15/2009

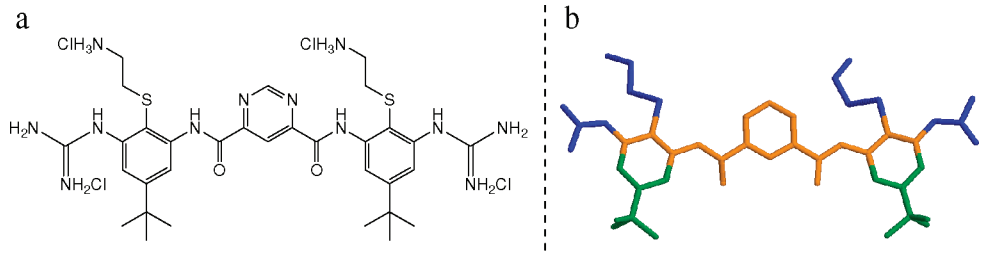

Figure 1. (a) Molecular structure of **1**, showing facial amphiphilicity. (b) Green groups below the central line of the molecule represent hydrophobic groups; blue groups above the central line of the molecule represent positively charged (hydrophilic) groups.

Solid-supported lipid bilayers have long been used as models for cellular membranes.[12] However, by many methods, studying a single lipid bilayer and any specific interactions between that bilayer and the molecules under study is extremely difficult as a direct result of the small amount of material involved. Bulky labels are often introduced to either the molecules interacting with the bilayer or the bilayer itself, which can have a dramatic effect on the system. Recently, SFG has been used to investigate lipid monolayers and bilayers with great success.[13−30] SFG has been used to monitor monolayer and bilayer structure, transmembrane movement of lipids, and transition temperatures of such solid-supported bilayers. Research has also shown SFG to be an extremely powerful technique in the investigation of bilayer−molecule interaction mechanisms, specifically because of its inherent surface specificity. For example, SFG studies on melittin interacting with bilayers indicated that melittin can adopt multiple orientations in a lipid bilayer.[18] Its interacting mechanisms or disrupting models depend on the melittin concentration. Time-dependent SFG studies have shown that the kinetics of melittin−lipid bilayer interactions are also determined by the melittin concentration.[15] The outer leaflet of the bilayer was disrupted first, followed by the second leaflet. Conversely, for tachyplesin I, both leaflets were disrupted simultaneously.[15]

In previously published research, this lab showed for the first time the details of the interaction between a single planar lipid bilayer functioning as a microbial membrane model and a novel membrane-active antimicrobial arylamide oligomer **1**.[11] These interaction details were determined in situ via SFG vibrational spectroscopy at concentrations around its minimum inhibitory concentration in real time. In this article, we expand upon that previous research, considering three different antimicrobial arylamide oligomers with significantly different activities.

EXPERIMENTAL SECTION

Solid-supported lipid bilayers were constructed using the Langmuir−Blodgett−Schaeffer method on CaF_2 right-angle prisms, as was done in our previous published research.[18] In each case, a hydrogenated proximal leaflet and a deuterated distal leaflet of the lipid bilayer were used to allow for independent monitoring of the C—H and C—D stretching ranges concurrently using SFG. Hydrogenated and deuterated 1,2-dipalmitoyl-*sn*-glycero-3-phosphoglycerol (DPPG and d-DPPG) were used to construct lipid bilayers to model bacterial membranes, as phosphatidylglycerol is the main component of the negatively charged lipids that make up bacterial cell membranes. Hydrogenated and deuterated 1,2-distearoyl-*sn*-glycero-3-phosphocholine (DSPC and d-DSPC) were used to construct bilayers to model mammalian membranes, as phosphocholine is a significant component of the zwitterionic mammalian cell membranes. In addition, phosphoethanolamine (PE), phosphocholine (PC), and phosphoglycerol (PG) mixtures were used in dye-leakage as well as SFG experiments. All lipids in this research were obtained from Avanti Polar Lipids (Alabaster, AL). Details regarding the antimicrobial experiments and dye leakage experiments are presented in the Supporting Information.

A neutral CaF_2 prism was used as the substrate rather than negatively charged mica or silica prisms, despite the more frequent use of the charged prisms. This was done to avoid the possible interactions between the positively charged oligomers and the mica or silica substrates. It was previously determined that these CaF_2 prisms are valid substrates for such supported bilayers.[11,15−18]

Details about the SFG theory, data analysis, and setup have been extensively discussed in previously published work[31−51] and will not be repeated here. Some details can be found in the

(12) Tamm, L. K.; McConnell, H. M. *Biophys. J.* **1985**, *47*, 105–113.
(13) Anderson, N. A.; Richter, L. J.; Stephenson, J. C.; Briggman, K. A. *J. Am. Chem. Soc.* **2007**, *129*, 2094–2100.
(14) Anglin, T. C.; Conboy, J. C. *Biophys. J.* **2007**, *95*, 186–193.
(15) Chen, X.; Chen, Z. *Biochim. Biophys. Acta* **2006**, *1758*, 1257–1273.
(16) Chen, X.; Boughton, A. P.; Tesmer, J. J. G.; Chen, Z. *J. Am. Chem. Soc.* **2007**, *129*, 12658–12659.
(17) Chen, X.; Wang, J.; Kristalyn, C. B.; Chen, Z. *Biophys. J.* **2007**, *93*, 1–10.
(18) Chen, X.; Wang, J.; Boughton, A. P.; Kristalyn, C. B.; Chen, Z. *J. Am. Chem. Soc.* **2007**, *129*, 1420–1427.
(19) Doyle, A. W.; Fick, J.; Himmelhaus, M.; Eck, W.; Graziani, I.; Prudovsky, I.; Grunze, M.; Maciag, T.; Neivandt, D. J. *Langmuir* **2004**, *20*, 8961–8965.
(20) Harper, K. L.; Allen, H. C. *Langmuir* **2007**, *23*, 8925–8931.
(21) Kim, J.; Kim, G.; Cremer, P. S. *Langmuir* **2001**, *17*, 7255–7260.
(22) Levy, D.; Briggman, K. A. *Langmuir* **2007**, *23*, 7155–7161.
(23) Liu, J.; Conboy, J. C. *J. Am. Chem. Soc.* **2004**, *126*, 8894–8895.
(24) Liu, J.; Conboy, J. C. *Biophys. J.* **2005**, *89*, 2522–2532.
(25) Ma, G.; Allen, H. C. *Langmuir* **2007**, *23*, 589–597.
(26) Nickolov, Z. S.; Britt, D. W.; Miller, J. D. *J. Phys. Chem. B* **2006**, *110*, 15506–15513.
(27) Ohe, C.; Sasaki, T.; Noi, M.; Goto, Y.; Itoh, K. *Anal. Bioanal. Chem.* **2007**, *3888*, 73–79.
(28) Sovago, M.; Wurpel, G. W. H.; Smits, M.; Muller, M.; Bonn, M. *J. Am. Chem. Soc.* **2007**, *129*, 11079–11084.
(29) Watry, M. R.; Tarbuck, T. L.; Richmond, G. L. *J. Phys. Chem. B* **2003**, *107*, 512–518.
(30) White, R. J.; Zhang, B.; Daniel, S.; Tang, J. M.; Ervin, E. N.; Cremer, P. S.; White, H. S. *Langmuir* **2006**, *22*, 10777–10783.
(31) Chen, Z.; Shen, Y. R.; Somorjai, G. A. *Annu. Rev. Phys. Chem.* **2002**, *53*, 437–465.
(32) Kim, J.; Somorjai, G. A. *J. Am. Chem. Soc.* **2003**, *125*, 3150–3158.
(33) Kim, G.; Gurau, M. C.; Lim, S.-M.; Cremer, P. S. *J. Phys. Chem. B* **2003**, *107*, 1403–1409.
(34) Oh-e, M.; Hong, S.-C.; Shen, Y. R. *Appl. Phys. Lett.* **2002**, *20*, 784–786.
(35) Ye, S.; Noda, H.; Nishida, T.; Morita, S.; Osawa, M. *Langmuir* **2004**, *20*, 357–365.
(36) Zhuang, X.; Miranda, P. B.; Kim, D.; Shen, Y. R. *Phys. Rev. B* **1990**, *172*, 303–306.

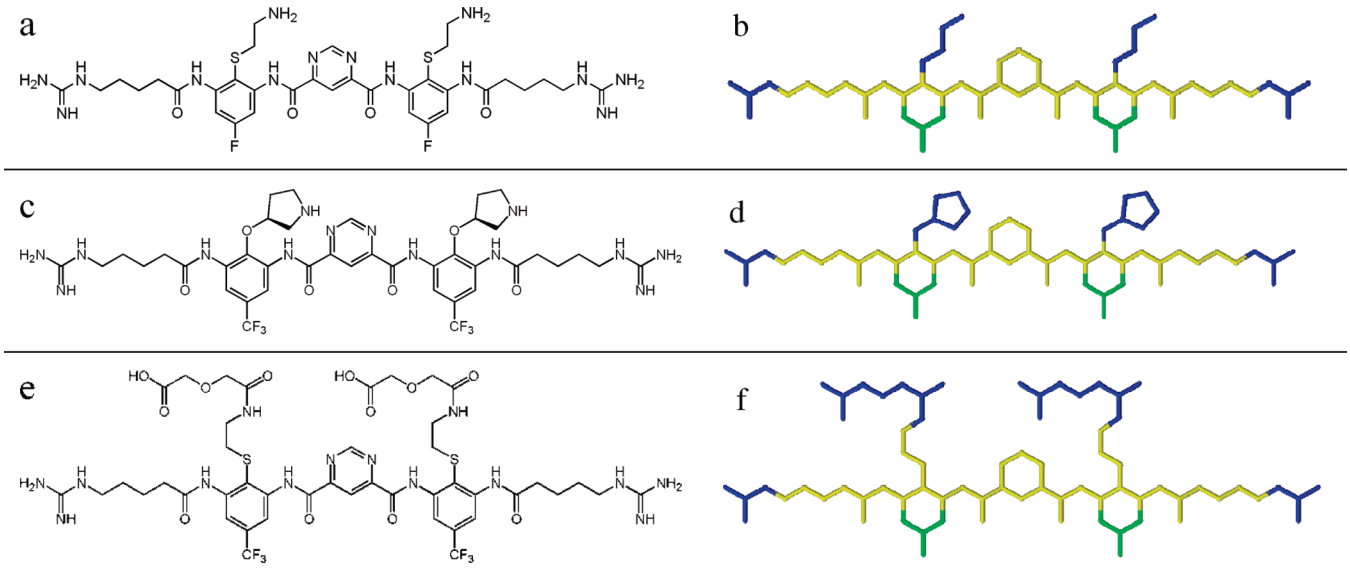

Figure 2. Oligomers **2** (a, b), **3** (c, d), and **4** (e, f). Blue sections represent positively charged functional groups and green sections represent hydrophobic portions of the oligomers. All oligomers share a common planar backbone structure, denoted in yellow.

Supporting Information. A total internal reflection geometry was used for all experiments performed in this research.[52] A polarization combination of s-polarized SFG output, s-polarized visible, and p-polarized IR beam (ssp) was used for virtually all SFG spectra discussed here. Spectra using a polarization combination of ppp (p-polarized SFG output, p-polarized visible, p-polarized IR) was used in concert with ssp to determine oligomer orientation in lipid bilayers.

RESULTS AND DISCUSSION

Our previous SFG studies on **1** (Figure 1) showed that the ability of **1** to interact with bacterial membrane models was strongly dependent on its concentration.[11] In these experiments, a DPPG (proximal leaflet)/d-DPPG (distal leaflet) bilayer was exposed to solutions of **1** with concentrations below, at, and above the minimum concentration required for bacterial growth inhibition (or minimum inhibition concentration, MIC). Isotopic labeling of the bilayer leaflets allowed the signals arising from the C—H and C—D stretches from the terminus of lipid chains in each leaflet to be independently monitored. At concentrations below MIC, the signal from the proximal leaflet remained constant, whereas the signal from the distal leaflet decreased. As the concentration was increased, the signal from both leaflets decreased to minimal levels, indicating the disruption of the lipid bilayer. Oligomer **1** was thus found to be capable to acting on the cellular membrane to kill bacteria, but that action is highly dependent on the compound's concentration. In addition, by comparing SFG signals arising from the CH_3 groups and C=O moieties located along the hydrophobic face of the oligomer using several polarization combinations of the input and output beams, we were able to determine the orientation of **1** while interacting with lipid bilayers. It inserts into the bilayer with a slight tilt from the surface normal, effectively making the oligomer more or less orient perpendicular to the lipid surface. It was this approximately perpendicular orientation that caused **1** to be referred to as a "molecular knife."

Oligomer Structures for the Current Study. Here, three new oligomers will be studied to understand the effect of the side chain identity on the membrane activity of the oligomer. As shown in Figure 2, these oligomers have a central delocalized core with guanidine side chains identical to the previously studied **1** but with different hydrophilic and lipophilic side chains. Fluoride and trifluoromethyl groups were used as lipophilic groups (different from compound **1**, which used *t*-butyl groups), and amino, guanidine, and carboxylic groups were used as hydrophilic groups. It is also worth noting that the side chains on some oligomers are more flexible than on others, with **4** having the largest amount of flexibility. This could have an effect on the activity and selectivity of the oligomer and should be considered in the design of these molecules.[8,9,53–62]

(37) Bain, C. D. *J. Chem. Soc., Dalton Trans.* **1995**, *91*, 1281–1296.
(38) Eisenthal, K. B. *Chem. Rev.* **1996**, *96*, 1343–1360.
(39) Wang, J.; Chen, C.; Buck, S. M.; Chen, Z. *J. Phys. Chem. B* **2001**, *105*, 12118–12125.
(40) Wang, J.; Paszti, Z.; Even, M. A.; Chen, Z. *J. Am. Chem. Soc.* **2002**, *124*, 7016–7023.
(41) Scatena, L. F.; Brown, M. G.; Richmond, G. L. *Science* **2001**, *292*, 908–912.
(42) Gautam, K. S.; Schwab, A. D.; Dhinojwala, A.; Zhang, D.; Dougai, S. M.; Yeganeh, M. S. *Phys. Rev. Lett.* **2000**, *85*, 3854–3857.
(43) Yang, C. S.-C.; Richter, L. J.; Stephenson, J. C.; Briggman, K. A. *Langmuir* **2002**, *18*, 7549–7556.
(44) Bordenyuk, A. N.; Jayathilake, H.; Benderskii, A. V. *J. Phys. Chem. B* **2005**, *109*, 15941–15949.
(45) Ma, G.; Liu, D. F.; Allen, H. C. *Langmuir* **2004**, *2004*, 11620–11629.
(46) Fitchett, B. A.; Conboy, J. C. *J. Phys. Chem. B* **2004**, *108*, 20255–20262.
(47) Ye, S.; Morita, S.; Li, G.; Noda, H.; Tanaka, M.; Uosaki, K.; Osawa, M. *Macromolecules* **2003**, *36*, 5694–5703.
(48) Kweskin, S. J.; Komvopoulos, K.; Somorjai, G. A. *Langmuir* **2005**, *21*, 3647–3652.
(49) Rivera-Rubero, S.; Baldelli, S. *J. Phys. Chem. B* **2004**, *108*, 15133–15140.
(50) Even, M. A.; Lee, S.-H.; Wang, J.; Chen, Z. *J. Phys. Chem. B* **2006**, *110*, 26089–27097.
(51) Baldelli, S. *Acc. Chem. Res.* **2008**, *41*, 421–431.
(52) Wang, J.; Even, M. A.; Chen, X.; Schmaier, A. H.; Waite, J. H.; Chen, Z. *J. Am. Chem. Soc.* **2003**, *125*, 9914–9915.
(53) Gabriel, G. J.; Maegerlein, J. A.; Nelson, C. F.; Dabowski, J. M.; Eren, T.; Nusslein, K.; Tew, G. N. *Chem.—Eur. J.* **2009**, *15*, 433–439.
(54) Som, A.; Vemparala, S.; Ivanov, I.; Tew, G. N. *Biopolymers* **2008**, *90*, 83–93.
(55) Som, A.; Tew, G. N. *J. Phys. Chem. B* **2008**, *112*, 3495–3502.

Table 1. Antibacterial Activity and Cytotoxicity of Oligomers 2, 3, and 4[a]

	MIC (μg/mL)		cytotoxicity	selectivity (EC_{50}/MIC)	
oligomer	*E. coli*	*S. aureus*	(EC_{50}, μg/mL)	*E. coli*	*S. aureus*
2	0.195	0.098	81	415	826
3	0.78	0.195	1031	1322	5287
4	>100	>100	>1000	N/A	N/A

[a] Cytotoxicity was evaluated in a colorimetric assay using a transformed human liver cell line (HepG2 cells).

Colorimetric assays were performed to determine activity, toxicity, and selectivity toward bacterial and mammalian cells. Oligomers **2** and **3** exhibited excellent antibacterial activity against *E. coli* and *S. aureus*; oligomer **4** remained inactive (as shown in Table 1). Although the antimicrobial activities of **2** and **3** are similar, **3** is significantly less cytotoxic toward mammalian cells resulting in superior selectivity indices (ratios of EC_{50} values for cytotoxicity to MIC).

Dye-leakage studies were also performed on **2**, **3**, and **4** to determine their activity toward bacterial and erythrocyte membrane models. Such experiments were done using four different liposomes having identical PG concentrations but different PE and PC concentrations (see more details about the experiments in Supporting Information). PE lipids are found at much higher concentrations in the bacterial cell membrane, while PC is widely distributed in erythrocyte membrane. Dye-leakage data from **2**, **3**, and **4** are shown in Figure 3A–C, respectively. Oligomer **2** remained active even at 40% PE lipid concentration, and its activity diminished as all the PE lipids were replaced by PC lipids. Oligomer **3** required more than 40% PE lipids in the outer leaflet to retain its activity. Oligomer **4** remained inactive against all lipid vesicles. Therefore, **2** was classified as active, **3** was classified as relatively selective, and **4** was classified as not active and not selective. The oligomers that were active enough to interact with PE and PG membranes should show a similar difference in SFG spectra, and those interactions were studied in the following experiments. With comparison to the dye-leakage experiment, SFG should be able to elucidate more molecular level information regarding the cell membrane (lipid bilayer)–oligomer interactions.

SFG Studies on Oligomers Interacting with DPPG Bilayer. Figure 4 shows the SFG spectra of a DPPG (proximal leaflet)/d-DPPG (distal leaflet) in both the C–H and C–D stretching regions. The spectrum a in Figure 4 shows the distal leaflet of the bilayer before contacting a solution of **2**. The dominant stretch comes at 2070 cm^{-1} and is due to the symmetric stretching of the terminal deuterated methyl groups in the d-DPPG leaflet. Spectra b, c, and d in Figure 4 were collected at increasing concentrations of **2**, until minimal signal from the distal leaflet could be detected. At the lowest concentration, 0.10 μg/mL, no decrease in SFG signal is observed. However, at higher concentrations, the observed signal drops dramatically. The greater the concentration, the greater the signal decrease. This is indicative of the oligomer partitioning into the bilayer and interacting with it. The decrease in signal from the distal leaflet should be due to disordering of the terminal deuterated methyl groups. While it is possible that this decrease could be due to displacement of the distal lipid molecules, it is unlikely. Light-scattering experiments were performed under similar conditions previously, and the results of those similar experiments (not reported in detail here) indicate that substantial destruction of the bilayer does not occur.

Spectra e–h in Figure 4 show the proximal leaflet of the same bilayer exposed to the same concentrations of **2**. The signals between 2800 cm^{-1} and 3000 cm^{-1} are primarily contributed by the methyl end groups of DPPG. The 2875 and 2940 cm^{-1} peaks are contributed by the symmetric C–H stretch and Fermi resonance of the methyl group. At the lowest concentration, 0.10 μg/mL, no change is observed in the proximal leaflet signal relative to the signal from the initial bilayer. As described previously, there was also no corresponding decrease in distal leaflet signal at this same concentration. Therefore, it seems that once the oligomer has reached a concentration at which it will interact with the bilayer, it affects both lipid leaflets at the same time. At higher concentrations there is significant decrease in both proximal and distal leaflet signals, indicating penetration of **2** into the inner leaflet. The concentration at which the oligomer begins disrupting bilayer SFG signals is around 0.25 μg/mL.

A similar study was done on DPPG/d-DPPG bilayers using increasing concentrations of **3**, the results of which are shown in Figure 5. In the case of **3**, the concentrations used ranged from 0.21 μg/mL to 1.2 μg/mL. As for **2**, a concurrent decrease in signal from the proximal and distal leaflets of the bilayer was observed. At the lowest concentration, signals from both leaflets remained unchanged, and at higher concentrations, a decrease in SFG signal from the proximal leaflet had a corresponding decrease in distal leaflet signal. A significant difference however was the range of concentrations needed to see the substantial and full disruption of the bilayer. There was only slight disruption for the DPPG leaflet when **3** reaches a concentration at 0.41 μg/mL (Figure 5h), while for **2**, a similar concentration (0.44 μg/mL, Figure 4d,h) completely disrupted both leaflets. Oligomer **3** substantially disrupts the DPPG leaflet when its concentration is at 0.82 μg/mL (Figure 5i). While **2** only needed approximately a third of the maximum concentration to substantially disrupt the DPPG leaflet (0.25 μg/mL, Figure 4g) comparing to that required for **3**. This is spectral evidence of a higher activity for **2** than **3**, which was also independently observed in dye-leakage tests previously described.

Oligomer **4** was studied in a similar way to **2** and **3**, however, with significantly different results, shown in Figure 6. DPPG/d-DPPG bilayers were exposed to much higher concentrations of **4** (maximum concentration was 5.8 μg/mL) relative to **2** or **3**; however, no SFG signal decrease was observed in either the C–D or C–H regions. This would indicate that **4** has no activity to this type of bilayer up to 5.8 μg/mL. Support for such a conclusion

(56) Scott, R. W.; DeGrado, W. F.; Tew, G. N. *Curr. Opin. Biotechnol.* **2008**, *19*, 620–627.
(57) Lienkamp, K.; Madkour, A. E.; Musante, A.; Nelson, C. F.; Nusslein, K.; Tew, G. N. *J. Am. Chem. Soc.* **2008**, *130*, 9836–9843.
(58) Gabriel, G. J.; Tew, G. N. *Org. Biomol. Chem.* **2008**, *6*, 417–423.
(59) Gabriel, G. J.; Madkour, A. E.; Dabowski, J. M.; Nelson, C. F.; Nusslein, K.; Tew, G. N. *Biomacromolecules* **2008**, *9*, 2980–2983.
(60) Ilker, M. F.; Nusslein, K.; Tew, G. N.; Coughlin, E. B. *J. Am. Chem. Soc.* **2004**, *126*, 15870–15875.
(61) Arnt, L.; Nusslein, K.; Tew, G. N. *J. Polym. Sci., Part A: Polym. Chem.* **2004**, *42*, 3860–3864.
(62) Arnt, L.; Tew, G. N. *J. Am. Chem. Soc.* **2002**, *124*, 7664–7665.

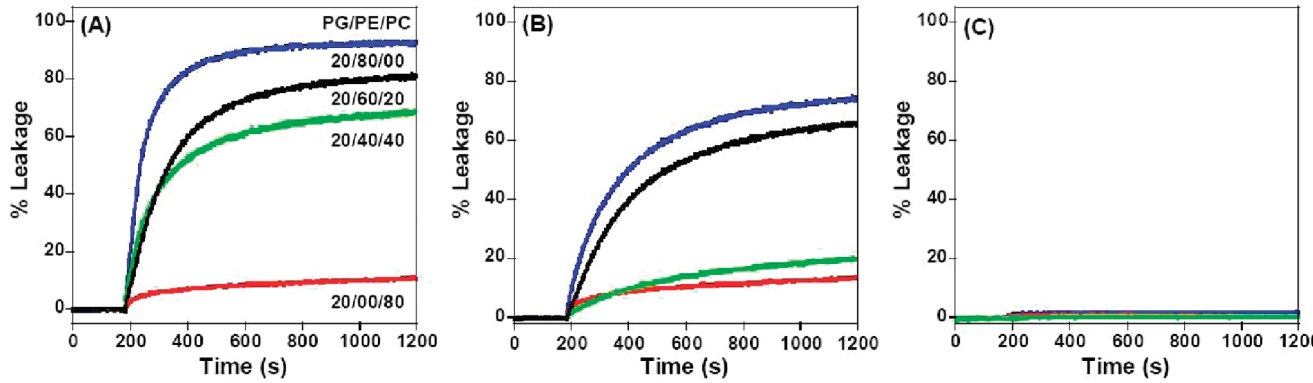

Figure 3. Percentage of calcein dye leakage from different DOPG/DOPE/DOPC liposomes having the same concentration of PG lipids and varied concentrations of PE and PC lipids. Oligomer **2**, plot A; **3**, plot B; **4**, plot C (DOPG/DOPE/DOPC: 20/80/00, blue; 20/60/20, black; 20/40/40, green; 20/00/80 red). The more selectively active oligomer **3** needed a higher percentage of DOPE lipids for its membrane activity. The dye leakage experiments were done in phosphate buffer, pH 7.0, at 2.0 μg/mL oligomer concentration (oligomer stock solutions were prepared in DMSO); final total lipid concentration is 5 μM.

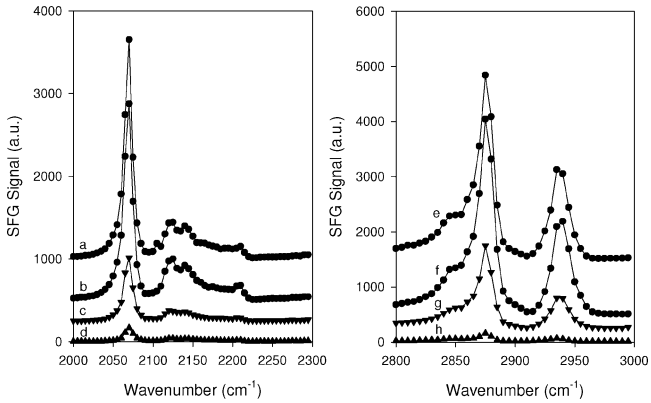

Figure 4. SFG spectra from a DPPG/d-DPPG bilayer in the C—D (left panel) and C—H (right panel) stretching regions before (a, e) and after being exposed to oligomer **2** at three solution concentrations: (b, f) 0.10 μg/mL; (c, g) 0.25 μg/mL; and (d, h) 0.44 μg/mL.

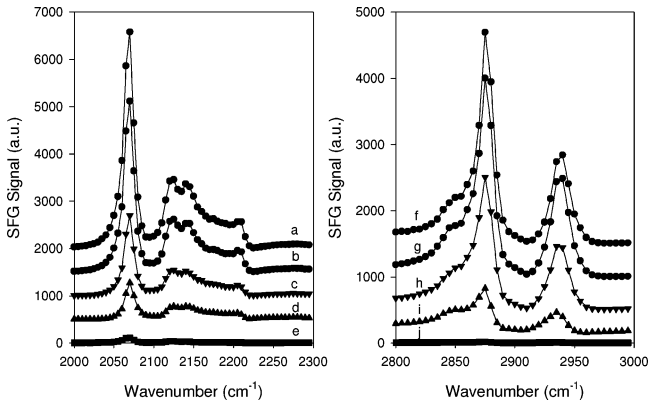

Figure 5. SFG spectra from a DPPG/d-DPPG bilayer in the CD (left panel) and CH (right panel) stretching regions before (a, f) and after being exposed to oligomer **3** at four solution concentrations: (b, g) 0.21 μg/mL; (c, h) 0.41 μg/mL; (d, i) 0.82 μg/mL; and (e, j) 1.2 μg/mL.

was also found in dye-leakage tests. As shown in Figure 3c, no dye leakage was detected for **4**.

Discussion on Possible Transmembrane Movements. One other possible explanation for the decrease in bilayer SFG signal in the cases of **2** and **3** could be the transmembrane movement of the lipids induced by these oligomers. Such flip-flop would mix

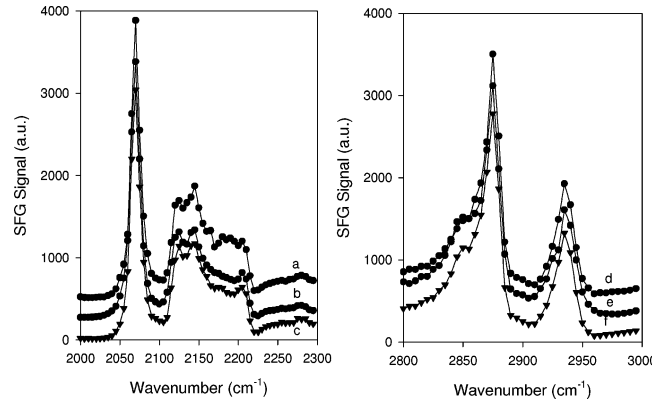

Figure 6. SFG spectra from a DPPG/d-DPPG bilayer in the CD (left panel) and CH (right panel) stretching regions before (a, d) and after being exposed to oligomer **4** at two solution concentrations: (b, e) 2.0 μg/mL; (c, f) 5.8 μg/mL.

the hydrogenated and deuterated lipids and result in reduced membrane asymmetry and thus a decrease in SFG signal. We believe that under the experimental conditions described here, these oligomers do not induce any significant transmembrane movement of lipids. For previously studied **1**, there was an independent decrease in signal from the proximal and distal leaflets. It was our contention that the different SFG signal decrease of the two leaflets of the bilayer after interacting with oligomers probably indicated that the SFG signal decrease was not primarily caused by the flip-flop. This type of signal was not observed in the case of the oligomers under study here, which saw a simultaneous decrease in SFG signals from both leaflets. The simultaneous decrease in signal could theoretically be from flip-flop among the leaflets. Under the current experimental conditions, the DPPG/d-DPPG bilayer should be in the gel phase, and the intrinsic flip-flop rate should therefore be negligibly slow when not interacting with the oligomers, as was observed (not shown). It has been found that when cell membranes interact with some antimicrobial peptides, transmembrane toroidal pores can be formed. Formation of transmembrane toroidal pores is known to greatly increase the flip-flop process by the creation of an aqueous channel by which polar headgroups can move from one leaflet to another without being forced to pass through the hydrophobic interior of the membrane. It is our belief that the

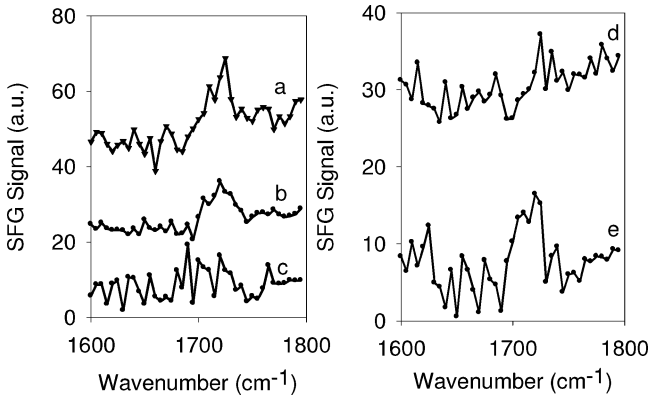

Figure 7. DSPC/d-DSPC bilayers exposed to high concentrations of oligomers **2** (left panel: (a) 19.9 μg/mL; (b) 9.9 μg/mL; (c) 2.38 μg/mL) and **3** (right panel: (d) 3.85 μg/mL; (e) 9.9 μg/mL). All concentrations are far above the concentration at which a DPPG membrane was disrupted.

oligomers, as small, relatively rigid molecules, are unlikely to form toroidal pore-like structures in a DPPG/d-DPPG bilayer. It is therefore most likely that these oligomers are directly disturbing the bilayer, rather than forming pore structures to cause flip-flop.

Oligomer Selectivity. As we discussed above, PG lipids are important components for bacterial cell membranes, while PC lipids are significant in mammalian cell membranes. Our previous studies on DPPC/d-DPPC bilayers indicate that the SFG C—H and C—D signals decrease very quickly even without interacting with any oligomers, due to the fast flip-flop (unpublished results). Therefore, it is difficult to study oligomer−DPPC/d-DPPC lipid bilayer interactions by observing SFG signal intensity decrease as we did when DPPG bilayers were used. Here, instead of using a DPPC/d-DPPC bilayer, we prepared a d-DSPG/DSPC bilayer, where no substantial flip-flop occurred. By using such a bilayer, for all three oligomers, even when the concentration is very high (e.g., ~20 μg/mL), no SFG signal decrease for the lipid bilayer was observed. This is correlated to the results shown in Figure 3 very well. As demonstrated in Figure 3, little dye leakage was observed when the oligomer concentration is at 5 μM for the liposomes containing 20% PG and 80% PC, relative to the other lipid mixtures tested.

To further investigate the selectivity of these oligomers between charged and neutral lipids, **2** and **3** were exposed to PC bilayers at higher concentrations, and SFG signals in the C=O stretching frequency region were monitored. The C=O signals can be contributed by both lipid bilayer head groups and the carbonyl moieties on the oligomer's planar core. However, the C=O signal from the oligomers is around 1705 cm^{-1}. According to our previous studies, the C=O signal from the lipid is centered at about 1720 cm^{-1}. They can be easily differentiated. Without the addition of oligomer, no C=O SFG signal was observed, showing that the lipid bilayer does not contribute to SFG C=O signals. The oligomer solutions with high concentrations were used to see if the oligomer could be forced to interact with the PC membrane at these higher concentrations. The collected spectra are shown in Figure 7. In the case of **2**, which is the less selectively active compound, a small amount of C=O signal can be seen in spectra a (with an oligomer concentration of 19.9 μg/mL) and b (with an oligomer concentration of 9.9 μg/mL) of Figure 7, however at a far lower level than seen for PG membranes, which will be shown below. Also, the concentration where these small signals were observed was at nearly 2 orders of magnitude higher than that required for PG membranes (see below). Similarly for **3**, small C=O signals can be seen at very high concentrations; however, they are again very small. These signals are around 1720 cm^{-1}. We believe that they are contributed by C=O signals from the lipid bilayer, due to the symmetry broken by small perturbations. Therefore, we conclude that at very high concentrations, these oligomers could be forced to interact with mammalian cell membranes to only a small degree. Shown later, the C=O signals observed in PG lipid membranes are centered at 1705 cm^{-1}, which should be dominated by the contributions from oligomers.

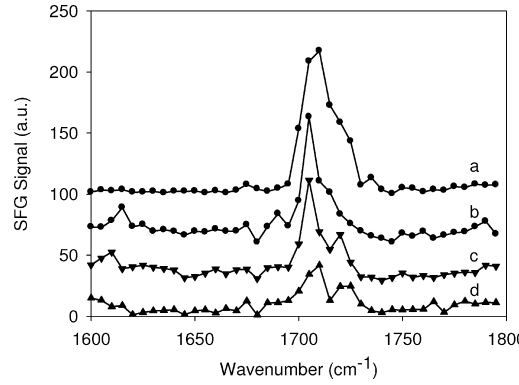

Figure 8. SFG spectra of d-DPPG/mixed (PG/PE/PC) bilayers exposed to 0.25 μg/mL of **2** (DPPG/DPPE/DPPC: (a) 20/80/0; (b) 20/60/20; (c) 20/40/40; (d) 20/0/80). Ratios are referenced to the percentage each lipid type has in the outer leaflet.

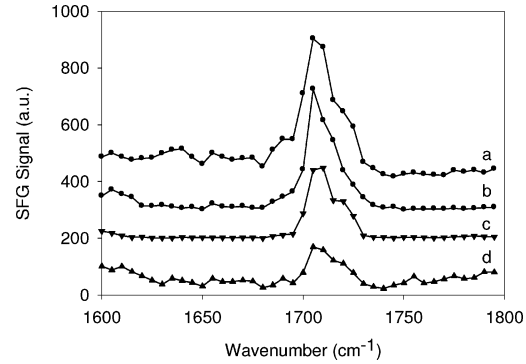

Figure 9. SFG spectra of d-DPPG/mixed (PG/PE/PC) bilayers exposed to 0.41 μg/mL of **3** (DPPG/DPPE/DPPC: (a) 20/80/0; (b) 20/60/20; (c) 20/40/40; (d) 20/0/80). Ratios are referenced to the percentage each lipid type has in the outer leaflet.

SFG Studies on DPPG/DPPE/DPPC Mixed Bilayers. To make a direct comparison between the dye-leakage test results and the SFG studies performed here, a study was done of DPPG/DPPE/DPPC mixed bilayers exposed to concentrations of **2** and **3**. Spectra are shown in Figures 8 and 9, respectively. In all cases, as the percentage of PC lipids in the outer leaflet increased, the C=O stretching signal (peaked at 1705 cm^{-1}) observed from the oligomer decreased. There is a significant decrease in signal from **2** when the %PE drops below 40%, and a similar decrease occurs for **3** when the %PE drops below 60%. Interestingly, the intensity of the C=O signal exactly follows the pattern observed

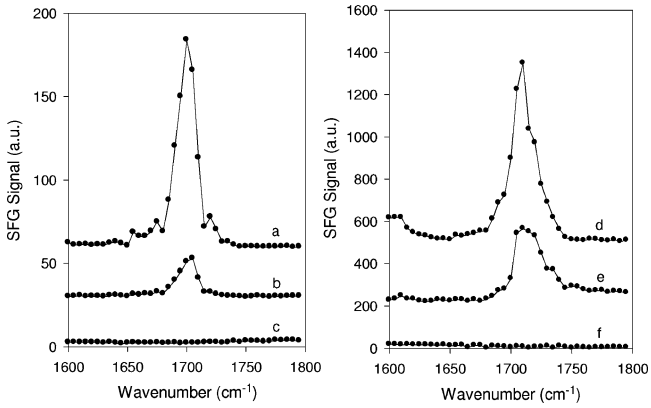

Figure 10. SFG spectra collected from a DPPG/d-DPPG bilayer in the CO stretching region. The left panel shows spectra of oligomer **2** at 0.25 μg/mL in (a) ppp, (b) ssp, and (c) sps polarization orientations. The right panel shows spectra of oligomer **3** at 0.41 μg/mL in (d) ppp, (e) ssp, and (f) sps polarization combinations.

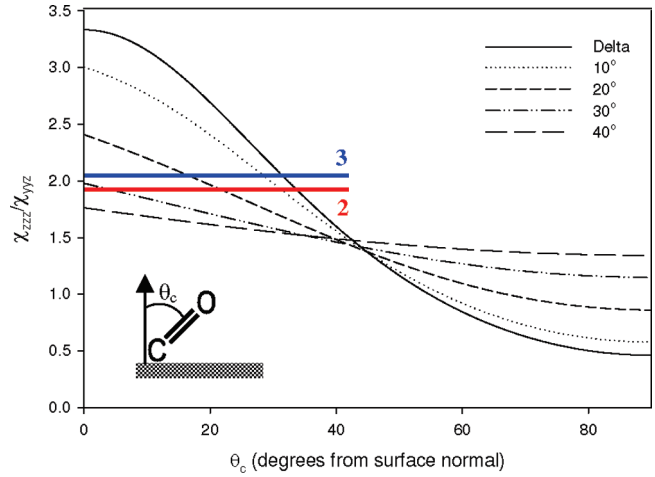

Figure 11. Relation between χ_{zzz}/χ_{yyz} and the orientation distribution of the parallel carbonyl groups. "Delta" means a delta-distribution, with orientation angle distribution width of 0°. For **2**, χ_{zzz}/χ_{yyz} was experimentally found to be 1.91, and for **3** it was found to be 2.05; this is indicated on the above plot by the red and blue bars, respectively.

in dye-leakage tests for these two compounds (Figures 3A,B). This would seem to imply that there is a significant correlation between the dye-leakage tests and our SFG results.

It is theoretically possible that the decrease in signal described above could be due to a reorientation of the oligomer upon interaction with the bilayer and not due to a lessened degree of interaction with PC lipids. To determine if this was a cause of the signal decrease, the orientation of the oligomers was determined using the method described further in this paper. In all cases, the orientation of the oligomers in the mixed bilayers was found to be identical to their orientation in DPPG/d-DPPG bilayers which will be reported later. It is therefore unlikely that the SFG signal decrease observed as the %PC of the bilayer increased was due to orientation changes of the oligomers. Details about the analysis of the orientation of these oligomers are discussed below.

It should be noted that all three sets of tests (exposure to PG bilayers, exposure to PC bilayers, and dye-leakage tests) all show similar results. In all cases, **2** is less selectively active than **3**, and **4** showed virtually no activity against any membrane type.

Oligomer Orientation. In the previous research, we have determined the orientation of **1** in the DPPG bilayer by collecting SFG C—H stretching signals from *t*-butyl groups.[11] It was found that **1** more or less stands up in the lipid bilayer, cutting the lipid bilayer as a molecular knife. Such an orientation was confirmed by C=O stretching signals collected using different polarization combinations of the input and output laser beams in the SFG experiment.[11] Since **2** and **3** do not have *t*-butyl groups, to determine their orientations inserted into the bilayer, orientational analysis of the C=O stretch (1705 cm^{-1}) of the carbonyl moieties on the oligomer was performed (Figure 10). Since a near total reflection geometry was adopted in the experiment, ppp spectra are mainly contributed by χ_{zzz}, while the contributions of χ_{xxz}, χ_{xzx}, and χ_{zxx} can be ignored, due to their negligible Fresnel coefficients.[63] From the ppp and ssp SFG spectra the χ_{zzz}/χ_{yyz} ratio can be deduced directly. According to the symmetry and hyperpolarizability of the C=O stretching mode, the χ_{zzz}/χ_{yyz} ratio of the C=O stretching mode as a function of different orientations and orientation distributions can be deduced,[64] as shown in Figure 11. The measured ratios are described by the red and blue bars for **2** (at 0.25 μg/mL) and **3** (0.41 μg/mL), respectively. As shown above, at these concentrations, **2** and **3** have similar disruption activities against PG bilayers. The measured χ_{zzz}/χ_{yyz} ratios for **2** and **3** are quite similar, corresponding to a more or less stand-up orientation (less than 35° from the bilayer surface normal) and a limited distribution width (less than 30°) for both oligomers. These results indicate that the plane of the oligomer is roughly perpendicular to the bilayer surface. This is the same method of interaction as was observed for **1**, which was found to insert into the bilayer approximately perpendicular to the bilayer plane. As mentioned, we have previously referred to this type of vertical insertion into the bilayer as a "molecular knife". If we compare **2** and **3**, **2** is only slightly less perpendicular to the lipid bilayer; however, the difference between **2** and **3** is so minimal it would seem to imply that the two oligomers orient approximately the same. Assuming that the distribution width is 30°, both **2** and **3** are approximately perpendicular to the lipid bilayer. As mentioned above, the orientation of the oligomers in the mixed bilayers was found to be identical to their orientation in DPPG/d-DPPG bilayers (details were not shown).

SFG C—F Stretching Signals. As mentioned, we deduced the orientation of **1** according to its *t*-butyl groups. Here **2**, **3**, and **4** do not have *t*-butyl groups but have some C—F groups instead. Research was previously conducted in this lab to investigate the spectrally observable effect a phenyl ring can have when attached directly to a trifluoromethyl group.[50] In those experiments, a strong coupling effect was observed between the CF_3 group and the phenyl ring, and the observation of SFG signal due to CF_3 stretches is highly dependent on that coupling. Those specific effects were observed from 4-(trifluoromethyl)benzyl alcohol (TFMBA); however, the comparison is still relevant here. As

(63) Nguyen, K.; LeClair, S.; Ye, S.; Chen, Z. *J. Phys. Chem. B* **2009**, *113*, 12169–12180.

(64) McClelland, A. Ph.D. Thesis, University of Michigan, Ann Arbor, MI, 2009.

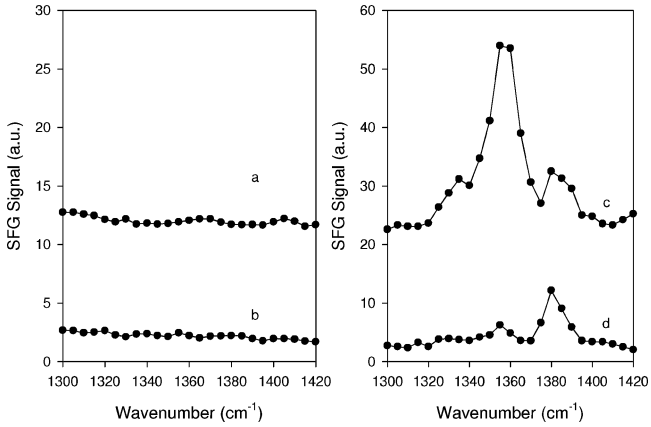

Figure 12. SFG spectra of CF stretching region for oligomers **2** (left panel) and **3** (right panel). Spectra a and c were taken in the ssp polarization combination whereas b and d were taken in ppp.

shown in Figure 2, **2** has a fluorine directly attached to two of the three phenyl rings, whereas **3** has a CF_3 group, just as in TFMBA. As can be seen in Figure 12, the SFG signal was detected in the CF stretching region for **3** and not for **2**. It is also worth noting that **4** also contains a CF_3 group attached to two of the three core phenyl rings. No CF SFG signal was detected from the lipid bilayer while in contact with the **4** solution. As previously discussed, **4** does not show any interaction to a DPPG bilayer and it does not goes to the interface, so we would therefore not expect to see any CF signal from **4** at the bilayer surface.

CONCLUSIONS

This paper investigates the mechanism of interactions between several AMP mimics and cell membrane models using SFG. By monitoring signals from C—H, C—D, C═O, and C—F stretches within the bilayer and the oligomer we were able to characterize and correlate results seen through SFG to dye-leakage, MIC, and colorimetric assay experiments. As with results from previous work, we were able to see disruption of the bilayer leaflets depending on oligomer concentrations. Three different oligomers have distinctly different activities against PG lipid bilayers. Oligomers **2** and **3** are quite active, while **4** is not. Oligomer **4** has a long and flexible polar/charged chain on one side of the molecule. This lack of rigidity of one side of the molecules may lead to its less active property. For **2** and **3**, while they interact with PG bilayers, they more or less stand up in the bilayer, as **1**. SFG studies indicated that under the oligomer concentrations we investigated, all three compounds are not active against PC lipid bilayers. Their activities and selectivities detected from SFG studies are well correlated to those observed from the dye-leakage, MIC, and colorimetric assay experiments. We believe that the detailed understanding of interactions between oligomers and cell membranes are critical to designing future methods of targeting bacterial cells without damaging human cells.

The methods described in this paper are also useful for investigating the interaction between solid-supported bilayers and larger proteins and peptides. Investigations into these types of interactions are currently underway in our lab. It is our belief that SFG is a powerful, unique, and very sensitive method for elucidating interactions such as those described in this paper. Fundamental studies of membranes and their associated biomolecules, as well as testing for effectiveness of antimicrobial peptides or antibiotic compounds, are necessary and critical to the pharmaceutical industry. We hope to develop SFG into a powerful bioanalytical tool.

ACKNOWLEDGMENT

This research is supported by the ONR (N00014-02-1-0832 and N00014-08-1-1211 for Z.C. and the ONR (N00014-07-1-0520) for G.T.

SUPPORTING INFORMATION AVAILABLE

Further details about sum frequency generation and fluorescence studies. This material is available free of charge via the Internet at http://pubs.acs.org.

Received for review June 11, 2009. Accepted August 22, 2009.

AC901271F